Chemical Science

ROYAL SOCIETY OF CHEMISTRY

EDGE ARTICLE

View Article Online
View Journal | View Issue

Cite this: *Chem. Sci.*, 2022, **13**, 13387

All publication charges for this article have been paid for by the Royal Society of Chemistry

Received 8th September 2022
Accepted 20th October 2022

DOI: 10.1039/d2sc05024b

rsc.li/chemical-science

Towards new coordination modes of 1,2,3-triazolylidene: controlled by the nature of the 1st metalation in a heteroditopic bis-NHC ligand†

Praseetha Mathoor Illam, Chandra Shekhar Tiwari and Arnab Rit *

An unusual effect of the nature of the first metal coordination of a heteroditopic N-heterocyclic carbene ligand (**L2**) towards the coordination behavior of 1,2,3-tzNHC is explored. The first metal coordination at the ImNHC site (complexes **3** and **4**) was noted to substantially influence the electronics of the 1,2,3-triazolium moiety leading to an unprecedented chemistry of this MIC donor. Along this line, the Rh^{III}/Ir^{III}-orthometalation in complexes **4** makes the triazolium C_4–H more downfield shifted than C_5–H, whereas a reverse trend, although to a lesser extent, is observed in the case of the non-chelated Pd^{II}-coordination. This difference in behavior assisted us to achieve the selective activation of triazole C_4/C_5 positions, not observed before, as supported by the isolation of the homo- and hetero-bimetallic complexes, **5**, **6** and **7**–**9** *via* C_5- and C_4-metalation, respectively. Furthermore, the $\%V_{bur}$ calculations eliminate any considerable steric influence and the DFT studies strongly support the selectivity observed during bimetalation.

Introduction

N-heterocyclic carbenes (NHCs), with their characteristic strong σ-electron donating nature[1] coupled with the tuneable stereo-electronic properties,[2] have proven to be a versatile class of ligands to anchor one, two or more metals for diversified applications.[3] Along with the very common Arduengo type imidazolylidenes, triazole derived 1,2,4-triazolylidenes have also been widely utilized for various applications.[4] After Bertrand's early discovery of 1,2,4-triazol-3,5-diylidene supported organometallic polymer,[5] the Peris group successfully utilized this bis-NHC system to access diverse homo- as well as heterometallic complexes.[3c,6] Later in 2008, the group of Albrecht introduced 1,2,3-triazolylidenes into the NHC family as an abnormal congener (mesoionic carbenes, MICs) of normal NHCs.[7] They exhibit superior donor properties, due to less heteroatom stabilization, which influence the reactivity of their transition metal complexes.[8] Furthermore, easy accessibility of the precursor triazolium salts *via* a simple [3 + 2] cycloaddition reaction of azides and alkynes ('click reaction')[8a,9] have made 1,2,3-triazolylidenes attractive in organometallic chemistry.[10] Among them, the 1,2,3-triazol-5-ylidenes derived from the corresponding C_4-protected triazolium salts are well explored,[10c,11] whereas the related MICs, generated from the analogous C_4- and C_5-unsubstituted triazolium salts, are rarely studied (Fig. 1).[12,13] This might be due to the availability of two backbone carbons (C_4 and C_5), which could, in principle, be deprotonated to yield either C_4- or C_5-ylidenes restricting the selective metalation.[12] This was indeed supported by the formation of a mixture of C_4- and C_5-coordinated products during the metalation of unsubstituted 1,2,3-triazolylidenes.[12] Moreover, the reported complexes of unsubstituted MICs are only of the cyclometalated type and they possess the metal center at the triazolylidene C_5-position (Fig. 1B).[12,13] The additional stability offered by chelation could possibly be the driving force for such metalation at the C_5-position.

Based on these literature reports, we engaged ourselves in developing strategies for selective activation of the backbone protons (C_4– and C_5–H) of the unsubstituted 1,2,3-triazolium salt as this will open up a new family of metal-NHC complexes for various applications including catalysis (activities of these regioisomeric metal complexes are expected to be different). We

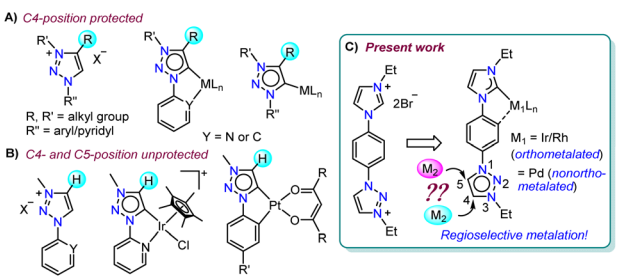

Fig. 1 Comparison of previous reports on 1,2,3-triazolylidene complexes with the present work.

Department of Chemistry, Indian Institute of Technology Madras, Chennai 600036, India. E-mail: arnabrit@iitm.ac.in

† Electronic supplementary information (ESI) available: Experimental details, characterization data, and NMR and mass spectra of the synthesized compounds. CCDC 2176097–2176105. For ESI and crystallographic data in CIF or other electronic format see DOI: https://doi.org/10.1039/d2sc05024b

hypothesized that either some electronic or steric modulation could help in achieving this. In this line, along with our interest[14a] towards hetero-bimetallic complexes,[14a,b] we have now designed an unsymmetrical bis-azolium salt [**L2**-H_2]Br_2 which possesses a triazolium group substituted with an *N*-phenyl-*para*-imidazolium moiety. The first metalation occurs at the imidazolium end as its C_2–H acidity is more compared to that of the triazolium backbone protons and thus, provides us the unique opportunity to control the subsequent metalation either at the C_4- or C_5-position of the triazolium group. Accordingly, monometalation of [**L2**-H_2]Br_2 with Pd^{II}- and Ir^{III}/Rh^{III} precursors yielded non-orthometalated (**3**) and orthometalated (**4a** and **b**) analogues, respectively which were detected to impart an unprecedented influence on the triazolium C_4/C_5–H chemical shifts and thus, essentially on their reactivities. This effect was utilized for the synthesis of their bimetallic counterparts (**5**, **6** from **3** and **7–9** from **4**) *via* selective activation of either the C_4– or C_5–H which was unequivocally supported by detailed NMR analyses along with the X-ray crystallographic studies.

Results and discussion

Previous reports on unsubstituted 1,2,3-triazolium salts with Ir^{III}- and Pt^{II}-centers[12,13] suggest that metalation occurs at the C_5-position of the triazole ring. However, it should be noted that these complexes are of the cyclometalated type which might have some influence on the metalation behavior. To understand this in detail, at the outset, we intended to study the chemistry of simple C_4/C_5-backbone unsubstituted mesoionic carbene precursors such as the click derived [**L1**-H]Br with Pd^{II} and Au^{I} centers (Scheme 1a) as they do not generally prefer the chelate complex formation *via* orthometalation. After synthesis, the NMR analyses of [**L1**-H]Br reveal that the C_4– and C_5–H resonances have very close chemical shift values (δ = 10.05 and 10.16 ppm, respectively), which might pose difficulties to its selective deprotonation cum metalation.

Nevertheless, [**L1**-H]Br was first reacted with [$Pd(CH_3CN)_2$-Cl_2] under suitable conditions (Scheme 1a) and the ^{1}H NMR spectrum with only one triazolylidene backbone proton along with a Pd^{II}-MIC $^{13}C\{^1H\}$ signal at δ = 139.5 ppm suggest the formation of a monopalladium complex. The X-ray crystallographic analysis disclosed the structure of complex **1** (Scheme 1b) in which the non-cyclometalated Pd^{II}-center is attached at the C_5-position of MIC ligand **L1**. To ascertain whether this is the preferred coordination mode of the ligand under consideration (**L1**) or not, we then attempted the synthesis of an analogous Au^{I}-complex (Scheme 1a). We first proceeded with the most common transmetalation strategy *via* Ag^{I}–NHC complex formation using Ag_2O. To our surprise, formation of a mixture of C_4- and C_5-ylidene coordinated Au^{I}-complexes[15] was observed even at room temperature, which could be due to the formation of both C_4– and C_5–ylidene coordinated Ag^{I}-complexes having similar stability and/or comparable carbene transfer efficiency.[12] This observation clearly suggests that both the backbone protons (C_4/C_5–H) are susceptible towards deprotonation. However, a C_5–ylidene coordinated Au^{I}-complex **2** was exclusively obtained in good yield (80%) *via* a Cs_2CO_3 assisted metalation strategy and the multinuclear NMR data along with the ^{1}H–^{1}H NOESY spectrum (Fig. S10†) confirmed the coordination of Au^{I} at the C_5-position of **L1**. This conclusion was established by the molecular structure determination *via* X-ray crystallography (Scheme 1b).

After studying the coordination behavior of the simple MIC ligand **L1**, we started investigating the possibilities of selective triazolium backbone activation. In this direction, as per our postulated electronic modulation, we designed an unsymmetrical bis-azolium salt [**L2**-H_2]Br_2, containing an imidazolium group along with a 1,2,3-triazolium moiety, the precursor for a biscarbene ligand. [**L2**-H_2]Br_2 was synthesized as an air stable white powder in excellent yield (94%) following the multistep procedure as detailed in Scheme 2. The ^{1}H NMR analysis reveals the most downfield shifted imidazolium N–CH–N proton resonance at δ = 10.20 ppm, whereas the two triazolium backbone N–CH–C protons were observed at δ = 9.79 (C_5–H) and 9.37 (C_4–H) ppm (confirmed by 2D NMR spectroscopy).

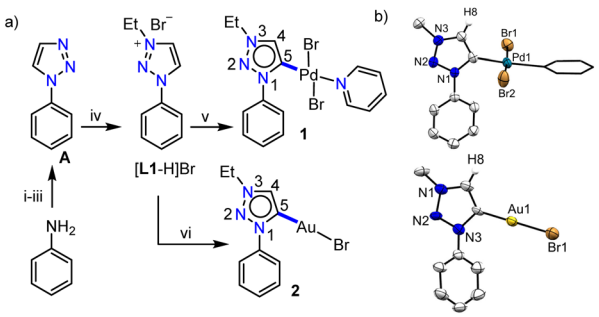

Scheme 1 (a) Synthesis of [**L1**-H]Br and its palladium (**1**) and gold (**2**) complexes: (i) $NaNO_2$, HCl/H_2O (10% solution), 0 °C, 1 h; (ii) NaN_3, 0 °C-RT, 12 h; (iii) vinyl acetate, reflux, 24 h; (iv) EtBr, CH_3CN, reflux, 24 h; (v) [$Pd(CH_3CN)_2Cl_2$], Cs_2CO_3, KBr, CH_3CN/pyridine, 70 °C, 24 h; (vi) [$Au(SMe_2)Cl$], Cs_2CO_3, CH_3CN, 70 °C, 24 h; (b) molecular structures of **1** and **2** with ellipsoids at a 50% probability level. Hydrogen atoms except H8 and Me moieties of the N–Et groups are omitted for clarity. Pyridine is shown in capped stick.

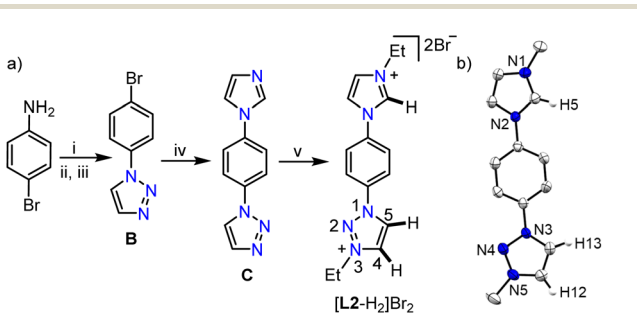

Scheme 2 (a) Synthesis of bisazolium salt, [**L2**-H_2]Br_2: (i) $NaNO_2$, HCl/H_2O (10% solution), 0 °C, 1 h; (ii) NaN_3, 0 °C–RT, 12 h; (iii) vinyl acetate, reflux, 24 h; (iv) imidazole, K_2CO_3, CuO, DMSO, 150 °C, 48 h; (v) EtBr, DMF, reflux, 24 h. (b) Molecular structure of [**L2**-H_2]Br_2 with ellipsoids at a 50% probability level. Hydrogen atoms except H5, H12, and H13, counterions, solvent of crystallization and Me moieties of the N–Et groups are omitted for clarity.

It is worth mentioning that the difference in chemical shifts of the triazolium backbone protons became more prominent after the installation of the imidazolium moiety in [**L2**-H_2]Br_2 as compared to that in [**L1**-H]Br. This indicates some electronic influence of the installed imidazolium moiety on the triazolium unit, which would probably be beneficial for the selective activation of its backbone protons. Moreover, the relatively higher acidity of the imidazolium N–CH–N proton than that of the triazolium ones implies that the first metalation should happen preferably at the imidazolylidene site, which would provide us with a unique opportunity to fine tune the electronics of the triazolium moiety *via* first metalation. Similar behavior was observed previously with a related unsymmetrical bis-azolium salt and was attributed to the difference in acidities[16a] of the azolium moieties.[16b] Finally, the structure of [**L2**-H_2]Br_2 was confirmed by X-ray crystallographic analysis (Scheme 2b).

With the well characterized bis-azolium salt [**L2**-H_2]Br_2 in hand, we proceeded to study its metalation behavior. Initially [**L2**-H_2]Br_2 was treated with [Pd(CH_3CN)$_2Cl_2$] in the presence of Cs_2CO_3 under the conditions shown in Scheme 3a. The NMR analyses confirmed the formation of complex **3** *via* coordination of a Pd^{II}-center to the imidazolylidene moiety, suggested by the absence of the most downfield shifted proton in the ^{1}H NMR spectrum as well as the Pd^{II}-bound ImNHC $^{13}C\{^1H\}$ NMR signal at $\delta = 150.2$ ppm.[17c,d] The chemical shift values of the backbone protons ($\delta = 9.92$ (C_4–H) and 10.24 (C_5–H) ppm) were assigned from the NOESY spectrum (Fig. S15†). Finally, the X-ray crystallographic analysis confirmed the coordination of Pd^{II} to the imidazolylidene donor (Scheme 3b). Before proceeding towards the synthesis of bimetallic complexes from **3**, we also synthesized the Ir^{III}-complex of [**L2**-H_2]Br_2, **4a**/**a**′ in good yields of 78–80%. The absence of the imidazolium proton of [**L2**-H_2]Br_2 and the observed integration of 3 instead of 4 aryl protons in the ^{1}H NMR spectrum along with the $^{13}C\{^1H\}$ NMR signal for the Ir^{III}-ImNHC at $\delta = 165.8$ ppm[17a,b] suggest the attachment of Ir^{III} to the imidazolylidene donor and the phenyl ring in an orthometalated fashion in complex **4a**. This is further substantiated by the diastereotopic nature of the imidazolium N–CH_2 protons (two multiplets of one proton intensity at $\delta = 4.24$ and 4.40 ppm). The X-ray crystallographic analysis of a single crystal of **4a**′ establishes the structure of the monoiridium complex (Scheme 3b) as concluded from NMR analyses. Interestingly, the 2D-NOESY (Fig. 2) spectrum of **4a** reveals that the triazolium C_4–H is significantly downfield shifted ($\delta = 9.86$ ppm) compared to C_5–H ($\delta = 9.05$ ppm).

In order to confirm this switching of triazolium backbone proton chemical shifts upon orthometalation, we also synthesized the analogous Rh^{III}-complex, **4b** (Scheme 3). The NMR analysis confirmed that the Rh^{III}-center also coordinates to the ImNHC in a similar way to Ir^{III} and importantly, has a comparable influence on the triazolium proton chemical shifts ($\delta =$ 9.83 and 9.09 ppm for C_4–H and C_5–H, respectively), in sharp contrast to that observed in the case of the non-orthometalated Pd^{II}-complex **3**. This may be attributed to the planar orthometalated Rh^{III}/Ir^{III}-center, which possibly attracts some electron density from the triazolium ring making the C_4–H more acidic than C_5–H.

All the above findings from the 1st metalation of ligand [**L2**-H_2]Br_2 ascertain that the nature of metal coordination offers substantial electronic influence on the triazolium moiety and thus, governs the chemical shifts, which would essentially control the activity of its backbone protons. It is in line with previous observations by several research groups that the coordination mode of a metal centre and its orientation after metalation strongly influence the site-selective C–H activation due to some electronic effect in the resulting system.[18]

With this definite idea about the electronic effect of the first metal coordination, we focused on the synthesis of the corresponding bimetallic complexes from **3** and **4**. First, the monopalladium complex, **3** was reacted with [Pd(CH_3CN)$_2Cl_2$] (Scheme 4a) and the product was isolated in good yield (85%). The NMR spectroscopic analyses provided primary evidence for

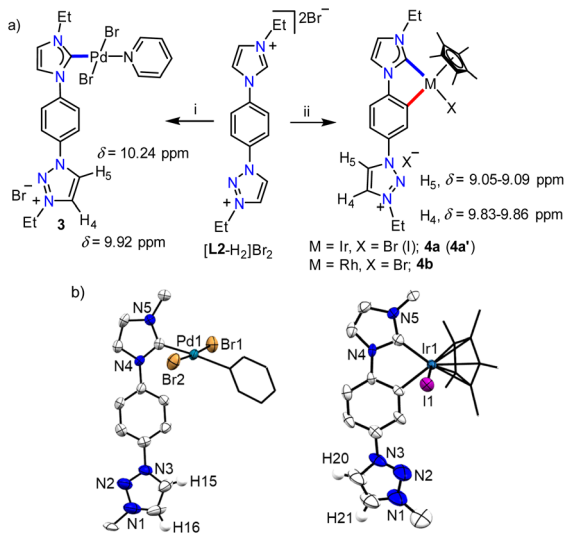

Scheme 3 (a) Synthesis of palladium (**3**), iridium (**4a** and **a**′), and rhodium (**4b**) complexes: (i) [Pd(CH_3CN)$_2Cl_2$], Cs_2CO_3, KBr, CH_3CN/pyridine, RT, 12 h. (ii) [M(Cp*)Cl_2]$_2$ (M = Ir/Rh), NaOAc, K_2CO_3/Cs_2CO_3, KBr (for **4a** and **b**) or KI (for **4a**′), CH_3CN, 75 °C, 24 h. (b) Molecular structures of **3** and **4a**′ with ellipsoids at 50% probability level. Hydrogen atoms except H15/H16 in **3** and H20/H21 in **4a**′, counter-ions, and the Me groups of N–Et moieties are omitted for clarity. Pyridine and Cp* moieties are shown in capped stick.

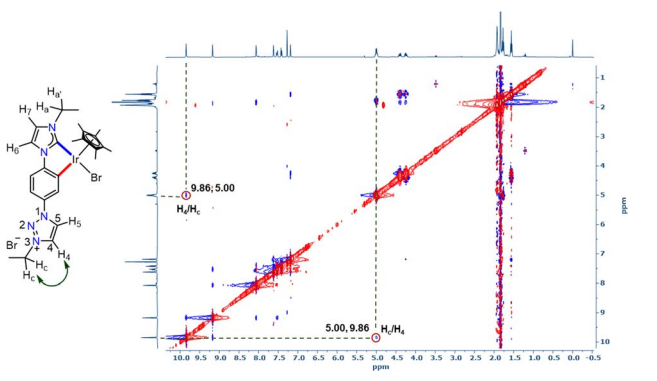

Fig. 2 2D-NOESY NMR spectrum of **4a** showing the interaction of triazolium C_4–H with the N–CH_2 protons of the ethyl group.

the homobimetallic complex (**5**) formation. First of all, the $^{13}C\{^1H\}$ resonances at $\delta = 150.6$ and 140.4 ppm, concluded to be Pd^{II}-ImNHC and Pd^{II}-MIC, respectively from the HMBC spectrum (Fig. S31†), confirm the attachment of two Pd^{II}-centers to ligand **L2**, which was also supported by the ESI-mass analysis. Furthermore, a resonance at $\delta = 7.74$ ppm in the ^1H NMR spectrum was assigned to the triazole backbone C_4–H based on the NOESY spectrum (Fig. S32†), indicating the Pd^{II}-coordination at the triazolylidene C_5-position. Finally, the single crystal X-ray crystallographic analysis confirmed the coordination of the second Pd^{II}-center to the C_5-position of 1,2,3-tzNHC (Scheme 4b), which was observed to have a more downfield shifted proton in **3** as per the detailed NMR analyses. To validate this further, we also synthesized another heterobimetallic (Pd^{II}–Au^{I}) complex **6** from **3** (Scheme 4) and the ^1H NMR spectrum of the obtained complex suggested the formation of the expected complex. Further support for the formation of the heterobimetallic complex, **6** was obtained from the ESI-MS analysis, exhibiting the most intense peak at m/z 729.8502 for $[M–Cl–py]^+$ (calcd. $m/z = 729.8540$) with the isotopic patterns matching perfectly. Coordination of Au^{I} to the 1,2,3-tzNHC C_5-position was finally established *via* single crystal X-ray crystallographic analysis of **6**. All the above results reinforce that the more downfield shifted triazolium proton is activated during the second metalation of a Pd^{II}–NHC complex (**3**) of $[L2\text{-}H_2]Br_2$.

Keeping this in mind, we proceeded with the second metalation of the orthometalated Ir^{III}-complex **4a** with the anticipated activation of the triazolium C_4–H. In this direction, complex **4a** was reacted with $[Pd(CH_3CN)_2Cl_2]$ using Cs_2CO_3 as the base in the CH_3CN/pyridine solvent mixture and the desired Ir^{III}–Pd^{II} bimetallic complex **7** was obtained in 64% yield (Scheme 5a). The ^1H NMR spectrum of **7** unveils that one of the triazolium protons of the precursor complex **4a** is missing as expected and the 2D NMR data confirmed the Pd^{II}-coordination to the C_4- instead of the C_5-position. This establishes the deprotonation of carbon having a more downfield shifted proton in **4a** during sequential metalation and notably, the C_5–H resonance is upfield shifted to $\delta = 7.93$ ppm in **7** from 9.05 ppm in **4a**. Furthermore, the attachment of Pd^{II} to the mesoionic carbene was supported by the $^{13}C\{^1H\}$ NMR carbene signal at $\delta = 136.3$ ppm, which was upfield shifted compared to the corresponding Pd^{II}-bound C_5-MIC signal at 140.4 ppm in **5**. Eventually, the X-ray crystallographic studies authenticate the attachment of Pd^{II} to the triazole C_4 position (Scheme 4b).

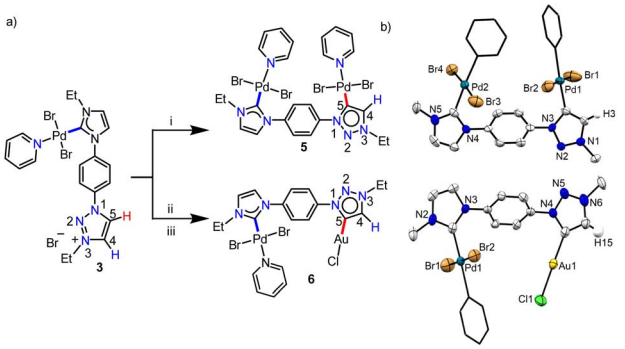

Scheme 4 (a) Synthesis of the bimetallic complexes **5** and **6** from **3**: (i) $[Pd(CH_3CN)_2Cl_2]$, Cs_2CO_3, KBr, CH_3CN/pyridine, 60 °C, 24 h; (ii) Ag_2O, DCM, RT, 12 h; (iii) $[Au(SMe_2)Cl]$, RT, 12 h. (b) Molecular structures of **5** and **6** with ellipsoids at a 50% probability level. Hydrogen atoms except H3 in **5**, H15 in **6**, and the Me groups of N–Et moieties are omitted for clarity. Pyridine groups are shown in capped stick.

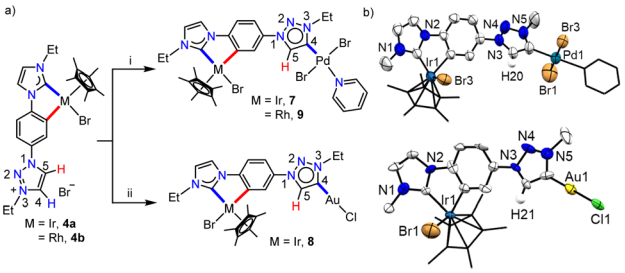

Scheme 5 (a) Synthesis of the heterobimetallic complexes **7–9**: (i) $[Pd(CH_3CN)_2Cl_2]$, Cs_2CO_3, KBr, CH_3CN/pyridine, 70 °C, 24 h. (ii) Ag_2O, DCM, RT, 12 h and then $[Au(SMe_2)Cl]$, RT, 12 h. (b) Molecular structures of **7** and **8** with ellipsoids at a 50% probability level. Hydrogen atoms except H20 in **7** and H21 in **8**, and the Me moieties of N–Et groups are omitted for clarity. Pyridine and Cp* moieties are shown in capped stick.

In order to affirm the activation of C_4- rather than the C_5-position of the triazolium moiety during the second metalation of the monoiridium complex **4a**, we further synthesized the related Au^{I} complex, **8** in 61% yield, following the transmetalation procedure (Scheme 5a). The HMBC spectrum, displaying a correlation of the Au^{I}-MIC $^{13}C\{^1H\}$ resonance with the Tz–N–CH_2 resonance (Fig. S41†), provides strong evidence for Au^{I}-coordination at the triazolylidene C_4 position which was ultimately established by the X-ray diffraction analysis (Scheme 5b). Furthermore, to prove the generality of this finding, we also utilized the mono-Rh^{III}-complex, **4b** for the synthesis of a Rh^{III}–Pd^{II} bimetallic complex **9** following a similar procedure used for the synthesis of complex **7** (Scheme 5). Multinuclear NMR spectroscopic along with mass spectrometric data analyses reveal the formation of the expected heterobimetallic complex, **9**. Moreover, the HMBC NMR spectrum (Fig. S45†) confirms the coordination of the Pd^{II}-center to the triazole C_4 position by exhibiting a correlation between the Pd^{II} bound tzNHC $^{13}C\{^1H\}$ signal at $\delta = 136.5$ ppm and the triazole Tz–N–CH_2 protons at $\delta = 5.09$ ppm, as observed in the case of the complex **7**. All of the above results establish that the orthometalated coordination of the Ir^{III}/Rh^{III}-center has a distinct electronic impact on the triazolium moiety in **4a** and **b** which plays a crucial role in achieving the selective activation of the triazole backbone C_4–H proton during the second metalation. It is worth mentioning that the complexes **7–9** represent the first ever isolated metal complexes of a C_5-unprotected 1,2,3-triazol-4-ylidene donor.

More insight into the contrasting influence of the 1st Pd^{II}- and Ir^{III}-metal centres on the second metalation was obtained from the $\%V_{bur}$ analysis and DFT calculations. The $\%V_{bur}$ calculated at the triazole C_5 position of the monometallic complexes, **3** and **4a′** was found to be essentially similar (50.1 *vs.* 50.4, calculated with a sphere radius of 3.5 Å, see the ESI†). This

observation clearly suggests that the selectivity observed during the formation of complexes **5**/**6** from **3** and **7**/**8**/**9** from **4** is primarily controlled by electronic factors. Furthermore, the difference of DFT calculated ground state energy between the representative bimetallic systems **5** with its C_4-analogue, **5′** and **7** with its C_5-analouge, **7′** was noted to be significant (0.7 kcal mol^{-1} and 1.4 kcal mol^{-1}, respectively, see the ESI†) and is in favour of the experimentally observed regioisomers. Thus, DFT calculations also endorse the isolation of C_5- and C_4-bound bimetallic systems (**5** and **7**, respectively) based on the nature of the 1st metal coordination to **L2**.

Conclusions

In conclusion, we have uncovered an unprecedented electronic influence of the 1st metal coordination on altering the reactivity/metalation behavior of the C_4/C_5-unprotected 1,2,3-triazolium moiety of a bis-azolium salt, [**L2**-H_2]Br_2. Importantly, the impact of monometalation in a non-chelated (complex **3**) or chelated (complexes **4a** and **b**) fashion on the triazole backbone (C_4/C_5) protons could be ascertained easily by 2D NMR analysis. Crucially, these changes in the electronic nature of triazole protons assisted us to access the first ever selective metalation at either the C_4- or C_5-position of 1,2,3-triazolylidene as undoubtedly supported by the synthesis of bimetallic complexes **5**–**9**. Furthermore, the $\%V_{bur}$ calculations suggest that the observed selectivity is primarily controlled by the electronic nature of the first metal coordination. Moreover, the DFT studies of selected complexes (**5** and **7**) strongly support the exclusive formation of a particular regioisomer as observed experimentally. The tandem catalytic activity studies of the synthesized complexes are underway in our laboratory.

Data availability

Experimental data including experimental procedures and characterization data (NMR, ESI-MS, and single crystal X-ray); the NMR and ESI-MS spectra of the new compounds; detailed computational studies are available in the ESI.†

Author contributions

A. R. conceived and designed the project. P. M. I. and C. S. T. performed the experiments. P. M. I. and A. R. wrote the manuscript and all authors approved the final version of the manuscript.

Conflicts of interest

There are no conflicts to declare.

Acknowledgements

We gratefully acknowledge SERB, India (Grant No. CRG/2020/000780) and IITM (IRDA) for financial support and the department of chemistry/SAIF, IIT Madras for the instrumental facility. P. M. I and C. S. T thank IIT Madras for a research fellowship. We also thank Dr P. K. S. Antharjanam and Mr Shashi Kumar for X-ray structure analyses and theoretical calculations, respectively.

Notes and references

1 For selected reviews, see: (*a*) D. Bourissou, O. Guerret, F. P. Gabbaï and G. Bertrand, *Chem. Rev.*, 2000, **100**, 39–91; (*b*) S. Diez-Gonzalez and S. P. Nolan, *Coord. Chem. Rev.*, 2007, **251**, 874–883; (*c*) D. L. Nelson and S. P. Nolan, *Chem. Soc. Rev.*, 2013, **42**, 6723–6753; (*d*) M. C. Jahnke and F. E. Hahn, Introduction to N-Heterocyclic Carbenes: Synthesis and Stereoelectronic Parameters, in *N-Heterocyclic Carbenes from Laboratory Curiosities to Efficient Synthetic Tools*, Royal Society of Chemistry, Cambridge, U.K, 2011, vol. 6, pp. 1–41.

2 For selected references, see: (*a*) R. Dorta, E. D. Stevens, N. M. Scott, C. Costabile, L. Cavallo, C. D. Hoff and S. P. Nolan, *J. Am. Chem. Soc.*, 2005, **127**, 2485–2495; (*b*) T. Dröge and F. Glorius, *Angew. Chem., Int. Ed.*, 2010, **49**, 6940–6952; (*c*) H. V. Huynh, *Chem. Rev.*, 2018, **118**, 9457–9492; (*d*) A. Gómez-Suárez, D. J. Nelson and S. P. Nolan, *Chem. Commun.*, 2017, **53**, 2650–2660.

3 (*a*) L.-A. Schaper, S. J. Hock, W. A. Herrmann and F. E. Kühn, *Angew. Chem., Int. Ed.*, 2013, **52**, 270–289; (*b*) R. Visbal and M. C. Gimeno, *Chem. Soc. Rev.*, 2014, **43**, 3551–3574; (*c*) J. A. Mata, F. E. Hahn and E. Peris, *Chem. Sci.*, 2014, **5**, 1723–1732; (*d*) S. Nayak and S. L. Gaonkar, *ChemMedChem*, 2021, **16**, 1360–1390; (*e*) F. E. Hahn and M. C. Jahnke, *Angew. Chem., Int. Ed.*, 2008, **47**, 3122–3172; (*f*) K. J. Evans and S. M. Mansell, *Chem.–Eur. J.*, 2020, **26**, 5927–5941; (*g*) N. Sinha and F. E. Hahn, *Acc. Chem. Res.*, 2017, **50**, 2167–2184; (*h*) R. C. Nishad and A. Rit, *Chem.–Eur. J.*, 2021, **27**, 594–599.

4 For selected references, see: (*a*) D. Enders, K. Breuer, G. Raabe, J. Runsink, J. H. Teles, J.-P. Melder, K. Ebel and S. Brode, *Angew. Chem., Int. Ed. Engl.*, 1995, **34**, 1021–1023; (*b*) D. Enders and K. Breuer, *J. Prakt. Chem.*, 1997, **339**, 397–399; (*c*) M. T. S. Metz, I. Münster, G. Wagenblast and T. Strassner, *Organometallics*, 2013, **32**, 6257–6264; (*d*) V. K. Singh, S. N. R. Donthireddy, P. M. Illam and A. Rit, *Dalton Trans.*, 2020, **49**, 11958–11970; (*e*) P. M. Illam and A. Rit, *Catal. Sci. Technol.*, 2022, **12**, 67–74.

5 O. Guerret, S. Solé, H. Gornitzka, M. Teichert, G. Trinquier and G. Bertrand, *J. Am. Chem. Soc.*, 1997, **119**, 6668–6669.

6 For selected references, see: (*a*) E. Mas-Marzá, J. A. Mata and E. Peris, *Angew. Chem., Int. Ed.*, 2007, **46**, 3729–3731; (*b*) A. Zanardi, J. A. Mata and E. Peris, *J. Am. Chem. Soc.*, 2009, **131**, 14531–14537; (*c*) S. Sabater, J. A. Mata and E. Peris, *Nat. Commun.*, 2013, **4**, 2553.

7 P. Mathew, A. Neels and M. Albrecht, *J. Am. Chem. Soc.*, 2008, **130**, 13534–13535.

8 For selected references(*a*) Á. Vivancos, C. Segarra and M. Albrecht, *Chem. Rev.*, 2018, **118**, 9493–9586; (*b*) D. Schweinfurth, L. Hettmanczyk, L. Suntrup and B. Sarkar, *Z. Anorg. Allg. Chem.*, 2017, **643**, 554–584; (*c*)

P. M. Illam, S. N. R. Donthireddy, S. Chakrabartty and A. Rit, *Organometallics*, 2019, **38**, 2610–2623.

9 (*a*) J. C. Sheehan and C. A. Robinson, *J. Am. Chem. Soc.*, 1951, **73**, 1207–1210; (*b*) R. Huisgen, *Angew. Chem., Int. Ed.*, 1963, **2**, 565–598; (*c*) S. N. R. Donthireddy, P. M. Illam and A. Rit, *Inorg. Chem.*, 2020, **59**, 1835–1847.

10 (*a*) K. F. Donnelly, A. Petronilho and M. Albrecht, *Chem. Commun.*, 2013, **49**, 1145–1159; (*b*) P. I. P. Elliott, *Organomet. Chem.*, 2014, **39**, 1–25; (*c*) G. Guisado-Barrios, M. Soleilhavoup and G. Bertrand, *Acc. Chem. Res.*, 2018, **51**, 3236–3244; (*d*) R. Maity and B. Sarkar, *JACS Au*, 2022, **2**, 22–57.

11 For selected references(*a*) G. Guisado-Barrios, J. Bouffard, B. Donnadieu and G. Bertrand, *Organometallics*, 2011, **30**, 6017–6021; (*b*) R. Maity, S. Hohloch, C.-Y. Su, M. van der Meer and B. Sarkar, *Chem.–Eur. J.*, 2014, **20**, 9952–9961; (*c*) L.-A. Schaper, L. Graser, X. Wei, S. J. Hock, A. Pöthig, K. Öfele, M. Cokoja, B. Bechlars, W. A. Herrmann and F. E. Kühn, *Organometallics*, 2013, **52**, 6142–6152; (*d*) E. C. Keske, O. V. Zenkina, R. Wang and C. M. Crudden, *Organometallics*, 2012, **31**, 6215–6221; (*e*) A. Bolje, S. Hohloch, D. Urankar, A. Pevec, M. Gazvoda, B. Sarkar and J. Košmrlj, *Organometallics*, 2014, **33**, 2588–2598; (*f*) R. Maity, A. Mekic, M. van der Meer, A. Verma and B. Sarkar, *Chem. Commun.*, 2015, **51**, 15106–15109.

12 A. Petronilho, J. A. Woods, H. Mueller-Bunz, S. Bernhard and M. Albrecht, *Chem.–Eur. J.*, 2014, **20**, 15775–15784.

13 (*a*) J. Soellner, M. Tenne, G. Wagenblast and T. Strassner, *Chem.–Eur. J.*, 2016, **22**, 9914–9918; (*b*) J. Soellner and T. Strassner, *Chem.–Eur. J.*, 2018, **24**, 5584–5590; (*c*) J. Soellner and T. Strassner, *ChemPhotoChem*, 2019, **3**, 1–6.

14 (*a*) R. C. Nishad, S. Kumar and A. Rit, *Organometallics*, 2021, **40**, 915–926; (*b*) H. Jin, T. T. Y. Tan and F. E. Hahn, *Angew. Chem., Int. Ed.*, 2015, **54**, 13811–13815.

15 The formation of a mixture of C_4/C_5-bound AuI-MIC complexes (in a 0.45:0.55 ratio), obtained by transmetallation of the *in situ* generated Ag-carbene complex of **L1**, was confirmed from the multinuclear (Fig. S46 and S47†) and 2D (HMBC) NMR data (Fig. S48†).

16 (*a*) E. M. Higgins, J. A. Sherwood, A. G. Lindsay, J. Armstrong, R. S. Massey, R. W. Alder and A.-M. C. O'Donoghue, *Chem. Commun.*, 2011, **47**, 1559–1561; (*b*) M. T. Zamora, M. J. Ferguson, R. McDonald and M. Cowie, *Organometallics*, 2012, **31**, 5463–5477.

17 (*a*) S. Semwal, I. Mukkatt, R. Thenarukandiyil and J. Choudhury, *Chem.–Eur. J.*, 2017, **23**, 13051–13057; (*b*) S. Semwal, D. Ghorai and J. Choudhury, *Organometallics*, 2014, **33**, 7118–7124; (*c*) T. Mondal, S. Yadav and J. Choudhury, *J. Organomet. Chem.*, 2021, **953**, 122047–122056; (*d*) C. J. Adams, M. Lusi, E. M. Mutambi and A. G. Orpen, *Chem. Commun.*, 2015, **51**, 9632–9635.

18 For selected references, see: (*a*) N. Hofmann and L. Ackermann, *J. Am. Chem. Soc.*, 2013, **135**, 5877–5884; (*b*) L. Ackermann, P. Novák, R. Vicente and N. Hofmann, *Angew. Chem., Int. Ed.*, 2009, **48**, 6045–6048.